A Statistical Investigation of Electron Radiation Belt Responses to High-Speed Solar Wind Stream Interfaces over a Range of L*-Values

S.K. Morley[1] ; R. H. Friedel[1]; E. Spanswick[1,2]; G. D. Reeves[1]; J. Koller[1]; T. E. Cayton[1]; E. Noveroske[1]

smorley@lanl.gov *(1- LANL, 2-U. Calgary)*

We present a statistical study of electron counts in the outer radiation belt across a range of L*-values (L*>4) combining data from over 7 CXD instruments, flown on the GPS constellation. The response of the relativistic electron data as functions of both time and drift shell are examined on a statistical basis for a set of high-speed solar wind stream interfaces; two-dimensional superposed epoch analysis is performed with the CXD data. For this set of epochs we study the variations in the electron radiation belts and in key geophysical parameters. We also present the first estimates of uncertainty in superposed epoch analysis.

FOR FURTHER DETAILS OF THE GPS CONSTELLATION, CXD DATA AND FAST RADIATION BELT LOSSES, PLEASE SEE REINER FRIEDEL'S POSTER (# SM23A-1598 ON TUESDAY)

Stream Interfaces

Stream Interfaces from high-resolution OMNI data

January 2005 – December 2008: 67 epochs
Epochs identified by concurrent:

- Jump in temperature
- Reversal in azimuthal flow velocity
- Increase in radial flow velocity
- Decrease in proton number density
- No subsequent interface within 1 day

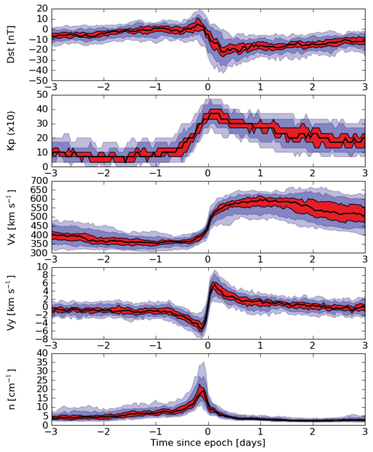

Figure 1: The superposed epoch median (black line), and 95% confidence interval (red band) of the Dst index (top panel), the solar wind radial velocity (second panel), the solar wind azimuthal velocity (third panel, GSE coordinates), and the solar wind proton number density. The blue bands mark the interquartile range (IQR; dark blue) and the 95% confidence interval about it.

The D_{st} index increases slightly prior to the epoch, coincident with the increased number density, and is depressed after the epoch. This is storm-like in form, but for ~70% of events Sym-H remains above -30nT. The median peak in Kp is 3^+.

Acknowledgements: The authors thank John Steinberg (LANL) and Joe Borovsky (LANL) for helpful discussions. Figures 1-5 inclusive were generated using the new SpacePy library in Python written by Steve Morley (under development at ISR-1, LANL).

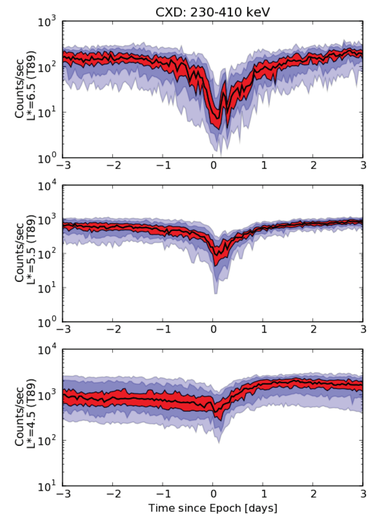

Figure 2: Superposed epoch plots of 230-410 keV CXD counts/sec at fixed L* (from top to bottom 6.5, 5.5, 4.5) for the set of stream interfaces. In each panel the black line marks the median and the red band shows the 95% confidence interval for the median. Similarly, the blue band marks the IQR and the lighter bands show the bounds of the 95% confidence interval for the IQR.

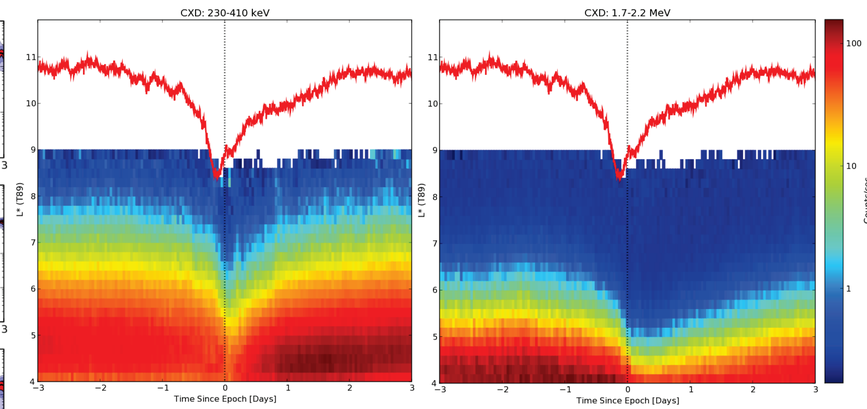

Figures 3 & 4: The superposed epoch median of CXD counts/sec for the set of stream interfaces, sorted by L* (calculated using T89 and the ONERA library). The resolution is 1-hr in time and 0.2 R_E radially. The red line shows the median standoff position from the Shue et al. [JGR,1996] magnetopause model.

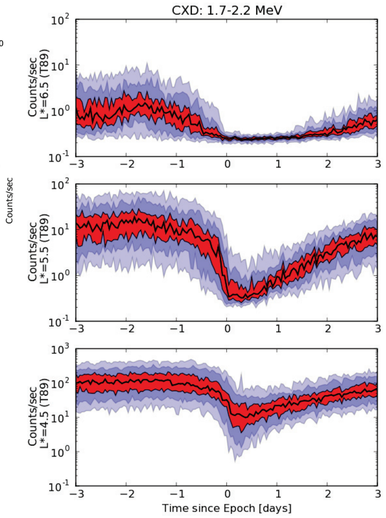

Figure 5: Same as figure 2, but for the 1.7-2.2 MeV energy channel. The confidence intervals were calculated using a bootstrapping technique detailed by Morley and Freeman [GRL, 2007].

Figures 2-5 show the central tendency of the superposed energetic electron data to magnetospheric driving by stream interfaces. The variability and uncertainty are displayed in figures 2 and 5. In the **230-410 keV** band we see a strong tendency to drop out at the arrival of the stream interface. The effect is less pronounced deeper in the magnetosphere. The electron counts tend to recover to pre-event levels inside a day. The median response at L*=4.5 is representative of the electron radiation belt inside of L*≈6, and shows a tendency to increased counts. The response in the **1.7-2.2 MeV** channel is different. Again a tendency to drop out is observed, which remains pronounced to L*=4. The recovery of these populations is also different. The timescale for recovery is much extended and appears to be slower at smaller L*.

It is also clear that the temporal evolution of the losses from the outer edge of the electron radiation belt are correlated with the median magnetopause standoff distance. This is also true for the estimated location of the last closed drift shell. A likely cause of the losses seen at and beyond geosynchronous orbit is a combination of outward radial diffusion and magnetopause shadowing.

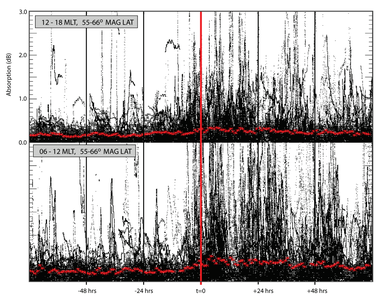

Figure 6: Superposed epoch plots of riometer data (North American and Scandinavian networks) for all epochs. All data are shown in black, the mean is shown by the red points. The upper panel shows the data for the afternoon sector and the lower panel shows the data for the morning sector.

Figures 6 and 7 show the absorption from riometers across the northern hemisphere. The absorption is shown as a latitudinal average in figure 6 and in bins of magnetic latitude and magnetic local time (MLT) in figure 7.

Absorption appears to increase (indicating the precipitation of >30 keV electrons) around the time of epoch, and the precipitation becomes more strongly organized ~3 hrs after the stream interface and peaks in the morning sector (9MLT;60-65MLat)

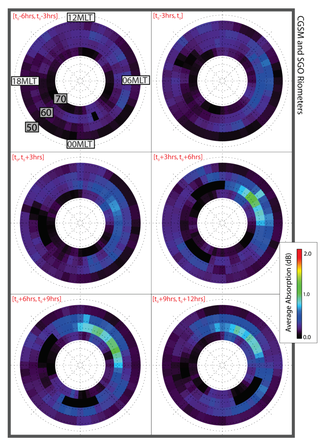

Figure 7: Maps of riometer absorption averaged over all 67 epochs, in 3 hour time bins.

Conclusions

- We have shown the first results of a statistical study of global in-situ measurements of radiation belt electrons using the GPS constellation.
- The central tendencies of radiation belt dropout and recovery are dependent on both L* and energy.
- For this set of stream interfaces, in ~70% of events Sym-H remains above -30nT, yet there is a strong tendency for radiation belt dropouts that penetrate to small L*. "Quiet-time" defined by D_{st}/Sym-H is not necessarily quiet!
- Precipitation around epoch is unstructured and bursty. From ~3 hrs after epoch precipitation is localized in the morning sector (approx. 5<L<6).